287

METEOROLOGICAL OFFICE

London Road, Bracknell
Berkshire RG12 2SZ

LONDON, METEOROLOGICAL OFFICE.
Met.O.11 Technical Note No.255

Strategies for using mesoscale data in an operational mesoscale model.

MET O 11 TECHNICAL NOTE NO 255

STRATEGIES FOR USING MESOSCALE DATA IN AN OPERATIONAL MESOSCALE MODEL

B.W. GOLDING

Meteorological Office, Bracknell, UK

Met O 11 (Forecasting Research)
Meteorological Office
London Road,
Bracknell
Berkshire
England.

March 1987

STRATEGIES FOR USING MESOSCALE DATA IN AN OPERATIONAL MESOSCALE MODEL

B W GOLDING

Meteorological Office, Bracknell, UK

ABSTRACT

Much of the success of experiments in mesoscale numerical weather prediction is due to the forcing of mesoscale disturbances by the synoptic scale flow and by the lower boundary. In such situations a good initialisation of the forcing is required, and also of the moisture field which normally provides the primary response. However more generally it is necessary to initialise the mesoscale circulations themselves. Current and planned observations of the required variables are inadequate so an indirect method based on the use of imagery is proposed with the following steps: classify the imagery, describe the structure, define the dynamical/thermodynamical processes, calibrate using all available data. Some of these steps are illustrated in two case studies.

Keywords: Mesoscale Forecasting Initialisation Models Imagery Clouds Fronts Fog

1. INTRODUCTION - MESOSCALE WEATHER PREDICTION

Several papers have appeared in recent years attempting to provide theoretical justification for definitions of mesoscale (Refs. 1-3). At one stage it was seen as the spectral gap between the synoptic scale and small scale turbulent eddies but it is now recognised that such a gap does not always exist. There is a degree of geostrophic control but the dynamics cannot be described in quasi-geostrophic terms. The vertical structure is mostly hydrostatically balanced but not entirely. Most importantly it is the scale on which most of the weather features that concern day-to-day human activities are found -

storms, fogs, frost pockets, cloud sheets etc.

The difficulty in extending conventional numerical prediction techniques to this scale is that the constraints operating at large scales are weakened giving the numerical models more freedom to deviate from the observed evolution. In microscale models and much mesoscale modelling, this problem is circumvented by restricting the range of problems studied. In many cases this adds new constraints to the model's freedom. Such constrained modelling has, however, demonstrated that a large proportion of mesoscale circulations are forced either by the large scale flow or by the lower boundary at the earth's surface. In the step to operational mesoscale weather prediction this provides a valuable guideline as to the sort of behaviour to expect from our models.

In making this step, we also have to solve the problem of specifying initial conditions in real time using routine observations. Here again, the constraints used in large scale model initialisation schemes in the form of balance equations etc. are of reduced validity. Also, whereas the models have the common framework of Newton's laws, it is not clear to what extent the general analysis theory developed for large scale models is applicable to the wider range of variables needed in mesoscale models. Finally it may be noted that the upper air observing network in the best observed regions of North America and Europe has a density relative to a 10 km mesoscale model mesh comparable with that in the southern hemisphere oceans for a global model before the introduction of satellite sounding.

2. THE MESOSCALE INITIALISATION PROBLEM

Since many mesoscale disturbances are forced either by the large scale flow or by the lower boundary, it is clearly necessary that this forcing should be correctly specified if a good forecast is to be obtained. So far as the large scale flow is concerned this requires a consistent specification of the temperature and velocity fields in the same way as for a large scale model. However, since very high accuracy of predicted position is required, this means that advecting velocities must be specified to a corresponding accuracy. In addition for a mesoscale model covering a small domain, this accuracy must also be present in the boundary conditions. Existing large scale models do not achieve sufficient accuracy in short period predictions of the position of features because their initial location and structure are inadequately defined by the observing network, especially over oceanic areas.

The specification of lower boundary forcing is a more complex problem since there are a number of contributing factors. Some such as orographic height and land/sea contrast are fixed and, in principle, can be specified to any required accuracy. The remaining problem here is to parametrize the effect of sub-grid scale variability. However, thermal forcing comparable with that at a coastline can also occur at the edge of a thick cloud sheet or of lying snow or even of moist ground. The correct representation of these is a prediction problem beyond a few hours ahead and certainly requires accurate specification of the moisture distribution in the atmosphere.

In both of these forced situations, the primary response of the atmosphere appears to occur through condensation of water and the consequent release of latent heat. The effects of this on the mesoscale structure of depressions and fronts (Refs. 4-6) have been well studied and its place in the development of convective systems (Ref. 7) is clearly central. Thus a detailed specification of the three dimensional moisture distribution is required for accurate prediction of the mesoscale response to forcing. In regions of near saturation this is well observed in the form of clouds both by human observers on the ground and by satellite imagery.

However, specification of the forcing and the moisture field is not sufficient for very short range forecasts. It may take several hours for a mesoscale disturbance to develop once the forcing starts. It is also necessary to predict the decay of a disturbance once the forcing ceases. For instance, an overnight forecast of a mesoscale convection system is unlikely to be very useful if it is initialised after sunset without such a system. Since the solar heating which generated it has stopped, there is unlikely to be any further development. This is where the problem of mesoscale initialisation reaches its most acute since such systems may not appear in any routine upper air sounding and yet their structures may be as complex as a synoptic scale depression. In general their structure is only routinely observable in satellite and radar imagery and this is the case because moisture not only plays an important part in generating them but it is also in the form of clouds and precipitation, their most discernible signature. In the absence of other data we must then ask whether the structure of mesoscale systems can in general be inferred from cloud and precipitation imagery. For initialisation of numerical models, this means not only associating conceptual models with the observed patterns, but also quantitatively defining their dynamics and themodynamics.

3. THE AVAILABLE OBSERVATIONS

Whereas large scale numerical models are very selective in their use of observations, it is both possible and necessary to use all types in mesoscale initialisation. In this section some of the characteristics of operational observing systems are considered so that their place in an initialisation strategy can be defined.

The radiosonde network has a target resolution of 300 km over land areas defined by the World Meteorological Organisation (Ref. 8) to meet synoptic scale forecasting requirements. This is met over most of Europe and North America. The frequency stated is 4 soundings per day. In both respects this is totally inadequate for mesoscale prediction. On the other hand, the vertical resolution obtained from radiosondes is good and in some countries excellent. The quality of temperature and wind soundings is also good but humidity data are of rather variable quality (Ref. 9). A characteristic of these data is that a full sounding takes over an hour and during this time the balloon may travel a hundred kilometres or more.

In large scale initialisation, satellite soundings are used to supplement the radiosonde network. These have a much better horizontal resolution where locally processed retrievals are available, although it is still coarser than that needed to define the structure of mesoscale systems. However, the vertical resolution is poor and uncertainly defined, especially near the ground. The sounding provides an area average appropriate to use in models but the accuracy depends on the retrieval technique used which may introduce biases towards mean or forecast conditions (Ref. 10). Satellite derived cloud motion vectors are available at few heights and with considerable uncertainty especially in midlatitudes.

Aircraft reports are currently made only in cruising flight and with poor resolution. They are mostly used to fill in gaps over the oceans.

The surface synoptic network has a density approaching that required for mesoscale analysis. A density of 1 station every 50 km and hourly reporting frequency are achieved in some areas. Observations of near surface quantities help to define the lower boundary condition for the upper flow. Cloud amount, base, type and precipitation observations give indirect information on the moisture distribution. Unfortunately these data are of variable quality, especially at night, depending on the skill and experience of the observer as well as the accuracy of his instruments.

Radar and satellite imagery are the only data available which can resolution of the prediction models. In the UK, composite radar rainfall maps are computed with a 5 km resolution every 15 minutes. Hourly Meteosat imagery is available with a resolution of about 5 km by 8 km and, when available, four polar orbiter images at 2 km resolution are available each day. A characteristic of these data is that they represent variables of little direct use to the model. Precipitation is a product of cloud but on its own is a diagnostic quantity. The cloud temperature is a useful input to defining the moisture distribution if it can be unambiguously assigned to a height in the atmosphere. As we shall see in section 4 this is not always possible. However, the patterns of cloud and precipitation contain valuable information about the processes that produced them, and it is the interpretation of those patterns either by human analyst or by expert system that provides the key to producing mesoscale analyses.

I have ignored future developments in remote sensing in this survey of observations for two reasons. Firstly, mesoscale numerical models are now being run operationally and so they need data now. Predictions of the available observations of tommorow must be set against predictions of tomorrow's models. Secondly, the history of satellite temperature sounding should make us cautious in expecting quick improvements in data availability, even where promising theory and technology already exist.

4. MODEL BASED INITIALISATION TECHNIQUES

In order to make use of the sort of technique outlined in sections 2, 3 a number of stages must be gone through. In summary these are

(i) classify mesoscale features observed in satellite and radar imagery

(ii) describe the qualitative structure of these features

(iii) define the dynamical and thermodynamical process operating in them

(iv) calibrate the model using all available data sources

In the case of synoptic scale systems the development of qualitative and dynamical understanding preceeded the use of imagery. Dynamical studies based on geostrophic scaling have a history of over 30 years and have led to the development of a number of calibration techniques including balance equations and normal mode initialisation (Refs. 11-13). The use of satellite imagery in this process has been developed chiefly in the southern hemisphere (Ref. 14) where there are less direct measurements. Here, the understanding of the structure of such systems has produced relationships between cloud features and the 1000-500 mb thickness pattern which are in routine use.

In frontal zones, geostrophic scaling is also proving useful in understanding smaller scale motions especially through use of the semigeostrophic approximation (Refs. 15-17). This promises to provide the dynamical framework for specifying the structure of such regions. The qualitative description of such structure is as old as the frontal models of the Bergen school itself and has received considerable attention in recent years (Ref. 18). Where large scale uplift is present we may be able to further simplify the dynamics to the extent that vertical motion is primarily forced by latent heat release. In this approach (Refs. 19, 20) a rainfall rate analysis, derived from imagery, is used to determine the amount of condensation and the consequent latent heating is applied with a predefined vertical profile over a period of integration at the start of the forecast. Specification of the heating profile is a problem but in principle it should be possible to use the model's precipitation physics. Unfortunately this approach cannot be used to correct errors in the rotational wind field or the temperature field since the adjustment period is too long.

Where synoptic scale influences are unimportant, the dynamics becomes rather easier. However in these situations the details of radiation and precipitation processes may make the initialisation problem just as difficult. As an example, for the cold sea fog described in section 4.2, studies indicate (Refs. 21-23) a common structure with an adiabatic temperature lapse and uniform wind within the fog. At fog top there is an inversion and wind shear over a shallow layer to match the ambient conditions above. Such a model provides a valuable framework for initialisation provided adequate data are available to classify it as a cold fog, to determine its coverage, and then to calibrate it with fog depth, surface wind, temperature and visibility and ambient wind and temperature above the inversion.

The next two sections illustrate some of the features of this approach to initialisation in the context of two case studies. The first is a cold front and the second a sea fog. The results are limited by the facilities available to perform the studies and by our understanding of the processes involved. They should not, therefore be seen as tests of the strategy.

4.1 Case Study - Cold Front 7/11/1986

This case study was chosen from the routine model forecasts because of a substantial timing error from early in the forecast. The UK Meteorological Office mesoscale model (Refs. 24-26) was used in its operational configuration with 15 km horizontal resolution and 16 levels, five of which are in the lowest kilometre. The non-hydrostatic equations are solved with a semi-implicit time scheme to retain stability of the sound waves. In routine use, a three hourly assimilation cycle incorporate forecasts from the UK Meteorological Office operational regional model (Ref. 27) to provide synoptic scale data (75 km resolution), and surface observations to provide boundary layer and cloud data. In this case, initial data were surface observations for 1800 GMT 7/11/1986, a three hour mesoscale forecast and a six hour regional forecast for the same time. A combination of the latter two provided the first guess and fig. 1 shows its representation of the surface pressure, wind and precipitation. The surface observations are plotted in fig. 2. Although the pressure trough and wind shear are well placed in fig. 1 being only a little too far east, the rainfall distribution is very poor with most of the rain ahead of the front. The observations show virtually no rain over England and Wales and this was confirmed by the radar. The objective analysis was able to remove the rain from ahead of the front but would not remove the erroneous deep layer of saturated air because of a cover of stratocumulus cloud ahead of the front which shielded higher levels from the surface observers.

A three hour forecast from these initial conditions is shown in fig. 3. Even in this short time, the rain has reformed ahead of the front and comparison with the observations in fig. 4 confirms that the forecast is seriously in error although the front itself is only a little fast. By six hours into the forecast, the forecast and observed rain areas scarcely overlap and the front itself is significantly too fast.

The main experiment performed with this case was to examine the impact of

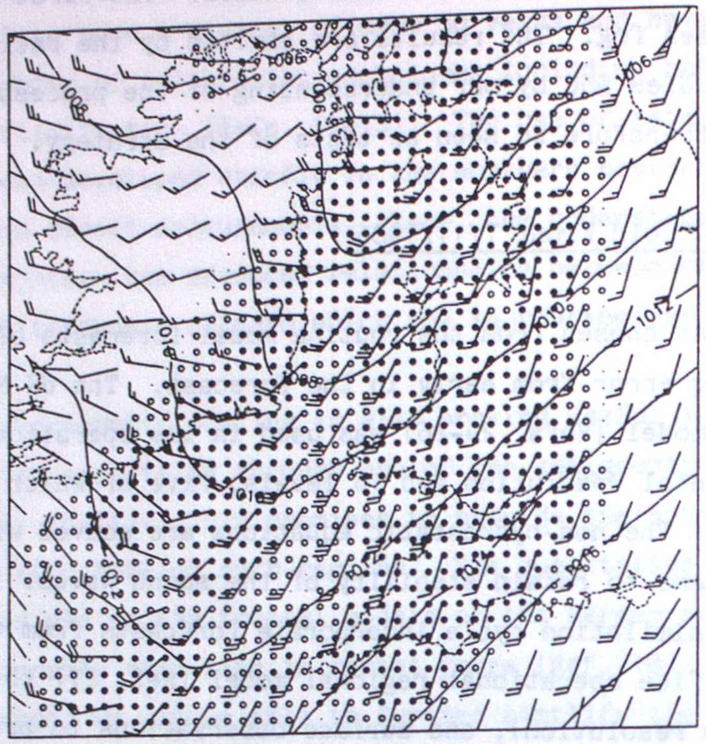

Figure 1. First guess surface pressure, wind and precipitation. 1800 GMT 7/11/1986. (·-drizzle, o-light rain, ● -moderate/heavy rain)

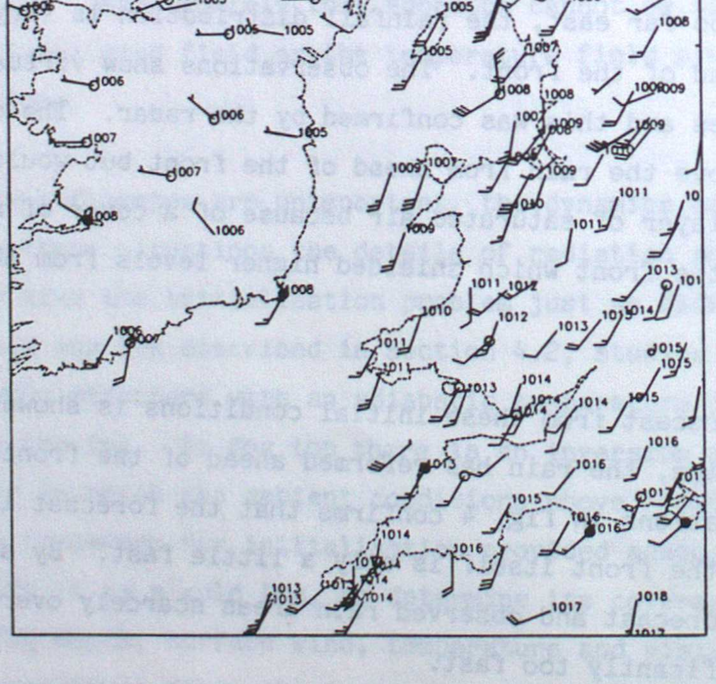

Figure 2. Observed surface pressure, wind and precipitation. 1800 GMT 7/11/1986. (o-light rain, ● -moderate/heavy rain, ∇ -light shower)

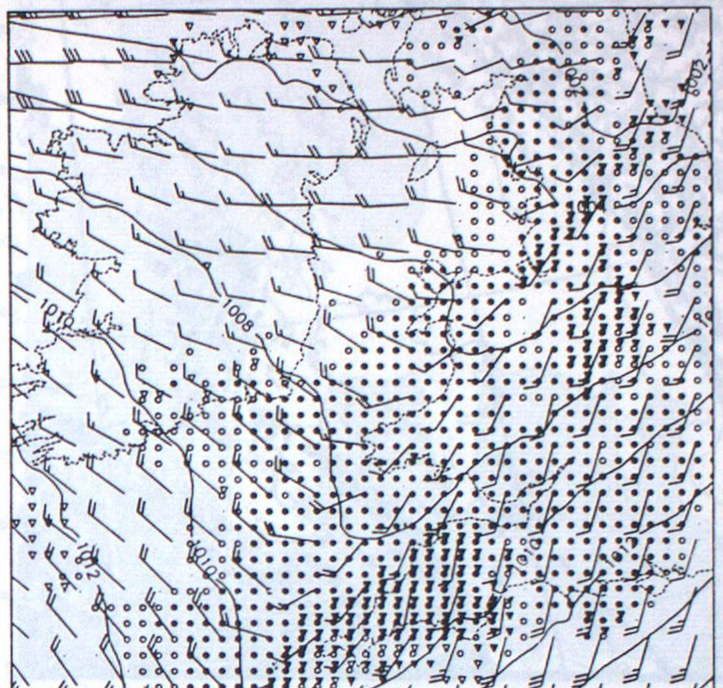

Figure 3. 3 hour forecast surface pressure, wind and precipitation from objective analysis. (·-drizzle, o-light rain, ● -moderate/heavy rain, ∇ -convective rain)

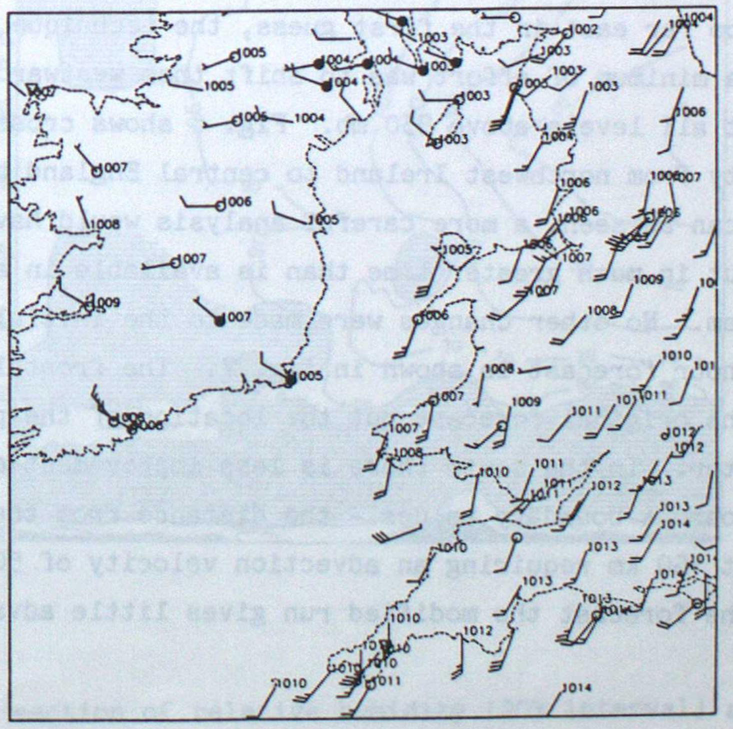

Figure 4. Observed surface pressure, wind and precipitation. 2100 GMT 7/11/1986. (o-light rain, ● -moderate/heavy rain, ∇ -light shower)

Figure 5. NOAA-9 infra red AVHRR image. 1400 GMT 7/11/1986. (Supplied courtesy of the University of Dundee)

removing the excess moisture ahead of the front. The satellite image in fig. 5 which was taken in the afternoon prior to analysis time confirms that only low cloud was present ahead of the front. Since the whole rainbelt appeared to be too far east in the first guess, the technique used to modify the fields with a minimum of effort was to shift them westwards by a prescribed amount at all levels above 850 mb. Fig. 6 shows cross sections of cloud and humidity from northwest Ireland to central England before and after the change. As can be seen, a more careful analysis would have produced better results but in much greater time than is available in a real time forecasting system. No other changes were made to the initial fields. The resulting three hour forecast is shown in fig. 7. The frontal position is unchanged from the original forecast but the location of the precipitation considerably better. In the south there is less improvement due to the advection of erroneous boundary values - the distance from the southern boundary is about 150 km requiring an advection velocity of 50 km hr^{-1}. By six hours into the forecast the modified run gives little advantage over the original.

A further experiment was performed in which the wind field was shifted westwards at all levels to try to correct the small error in frontal position.

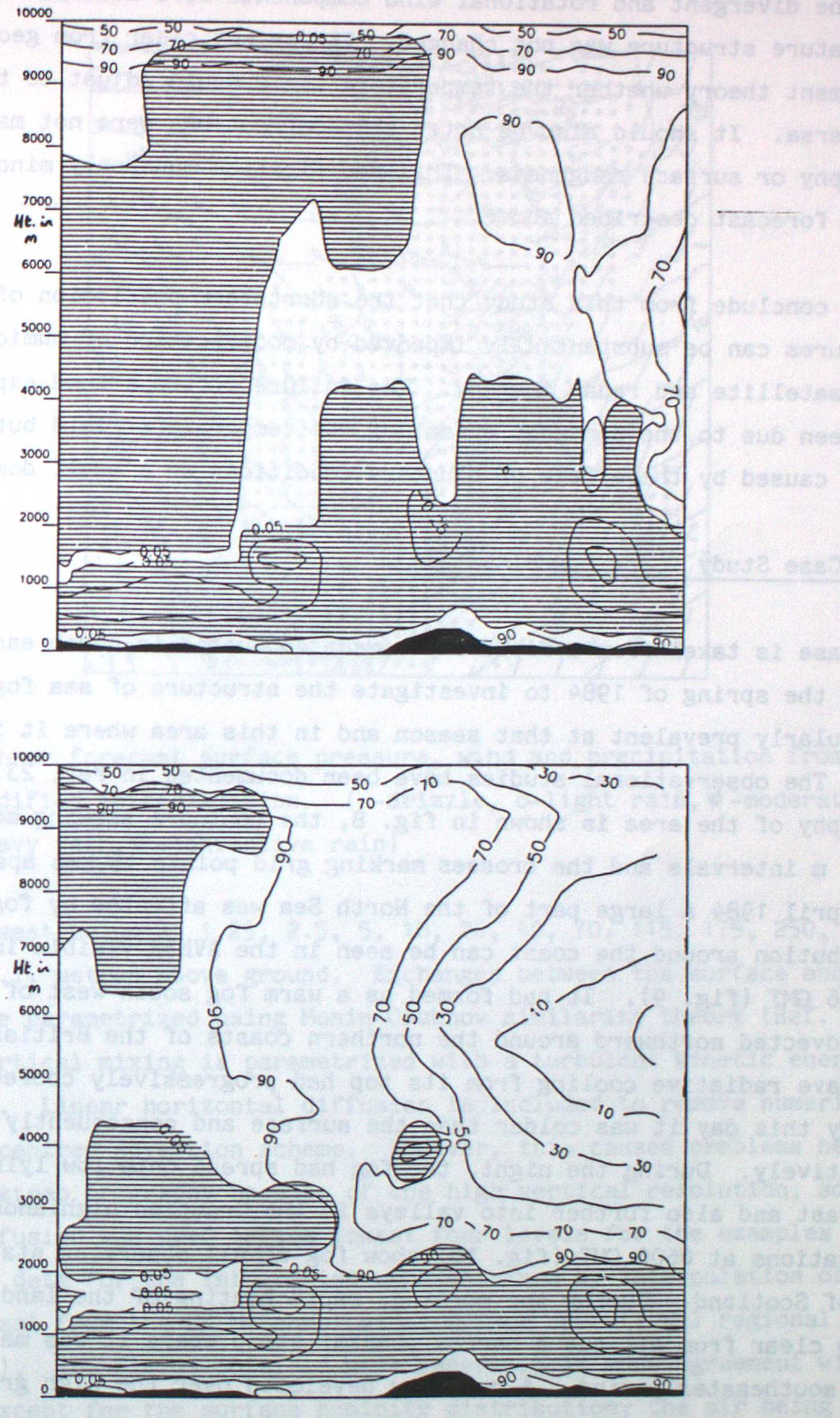

Figure 6. Cross section of relative humidity (20% interval) and cloud water (shaded, 0.2 gkg^{-1} interval)

a) objective analysis

b) after modification

Both the divergent and rotational wind components were modified but the temperature structure was not changed. It was not clear from geostrophic adjustment theory whether the temperature field would adjust to the winds or vice versa. It should also be noted that corrections were not made for the orography or surface roughness. This modification made only minor differences to the forecast described above.

We may conclude from this study that the short term prediction of frontal structures can be substantially improved by modification of humidity fields using satellite and radar imagery. The failure of the second experiment may have been due to the dominant effect of the temperature field but was more likely caused by the effect of boundary conditions on a small domain.

4.2 Case Study - Sea Fog 27/4/1984

This case is taken from a field experiment conducted in north east Scotland during the spring of 1984 to investigate the structure of sea fog which is particularly prevalent at that season and in this area where it is known as Haar. The observational studies have been documented in ref. 23. The geography of the area is shown in fig. 8, the contours showing model terrain at 100 m intervals and the crosses marking grid points 15 kms apart. On 27th April 1984 a large part of the North Sea was affected by fog and its distribution around the coast can be seen in the AVHRR visible image taken at 1446 GMT (fig. 9). It had formed as a warm fog south west of Ireland and been advected northward around the northern coasts of the British Isles. Long wave radiative cooling from its top had progressively cooled the fog so that by this day it was colder than the surface and consequently well mixed convectively. During the night, the fog had spread onto low lying land near the coast and also further into valleys in the Grampian highlands. Surface observations at 0600 GMT (fig. 10) show fog at all observing stations in the east of Scotland. During the morning, rapid heating of the land caused the fog to clear from all but a narrow coastal strip where it was maintained by a light southeasterly wind. A heat low developed over the high ground and generated a wind circulation assisting the maintenance of coastal fog except on the southern side of the Moray Firth as can be seen in the satellite image, fig. 9 and the surface observations for 1500 GMT, fig. 11.

A version of the UK Meteorological Office mesoscale model with enhanced vertical resolution was used for simulations of this case. It had twenty-nine

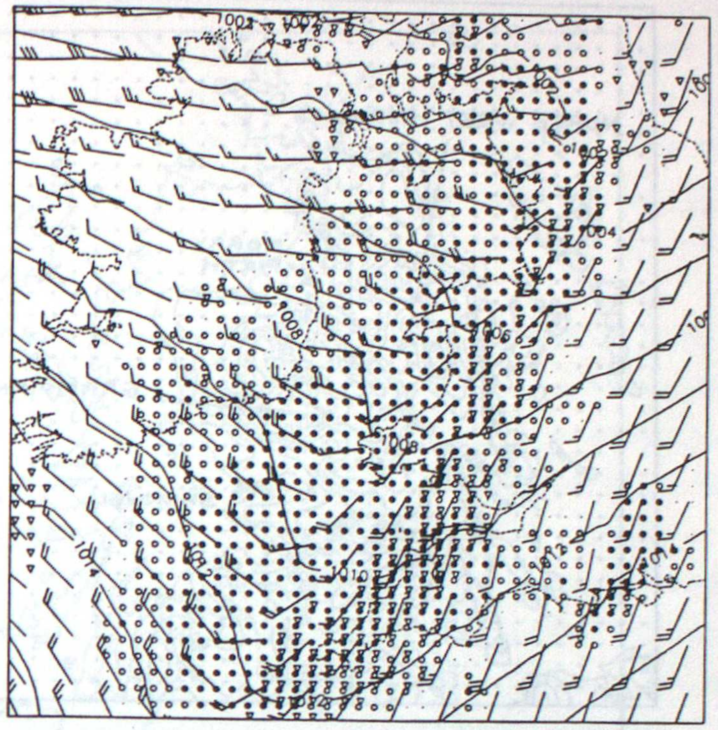

Figure 7. 3 hour forecast surface pressure, wind and precipitation from modified initialisation. (· -drizzle, o-light rain, ● -moderate/heavy rain, ∇ -convective rain)

levels, the lowest being at 1.25, 2.5, 5, 10, 20, 40, 70, 115, 175, 250, 340, 445, 565, 700 ... metres above ground. Exchanges between the surface and first level are parametrized using Monin-Obukhov similarity theory (Ref. 25). Above this, vertical mixing is parametrized with a turbulent kinetic energy closure scheme. Linear horizontal diffusion is included to remove numerical errors in the centred advection scheme. However, this caused problems near the ground in steep orography because of the high vertical resolution, so no horizontal diffusion was used in the lowest four levels for the examples shown here. Initial data for the integration were obtained by interpolation of a six hour forecast from the UK Meteorological Office operational regional model (Ref. 27). The fields obtained were generally in good agreement with observations except for the surface humidity distribution, the air being too dry over the North Sea and too moist to the west of Scotland. Without a correct initial distribution of fog it is not surprising that the nine hour forecast (fig. 12) is incorrect. Over the Highlands where the fog cleared quickly, the predicted temperatures are in good agreement with observations (fig. 11) but on the east coast the lack of fog or low cloud has allowed higher temperatures to develop than were observed.

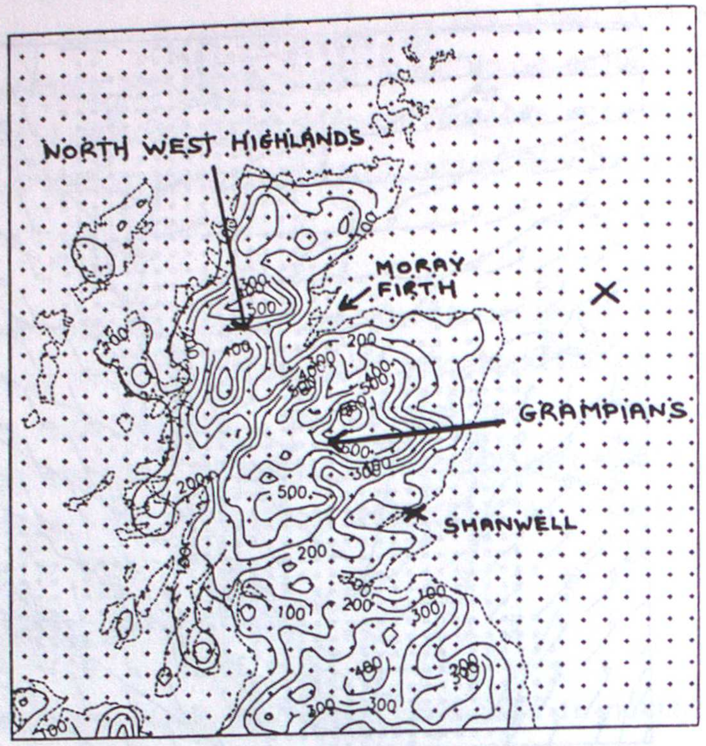

Figure 8. Topography of Scotland. Model grid points and orography (100 m interval)

Figure 9. NOAA-7 visible AVHRR image. 1448 GMT 27/4/1984 (supplied courtesy of the University of Dundee)

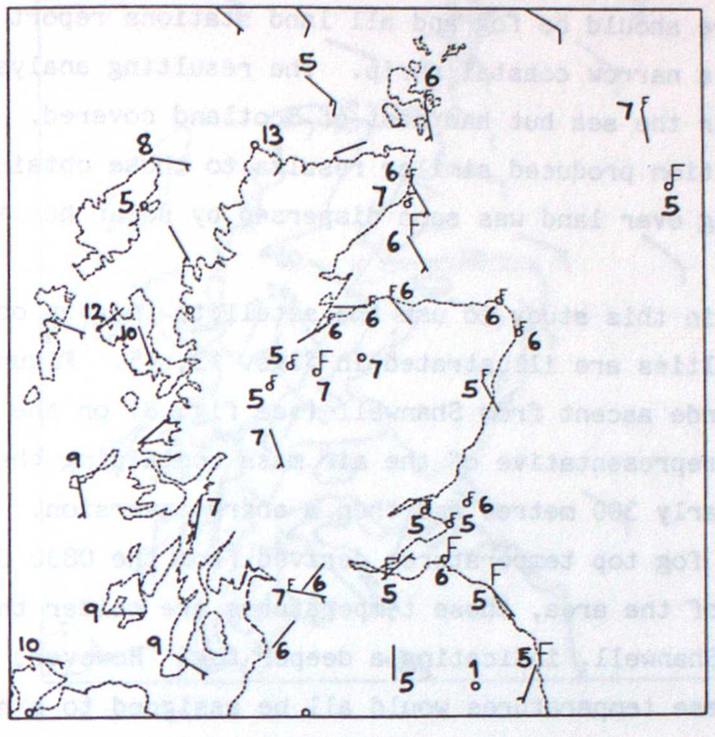

Figure 10. Observed temperature, wind and fog 0600 GMT 27/4 1984. (F-visibility <200 m, f-visibility <1000m)

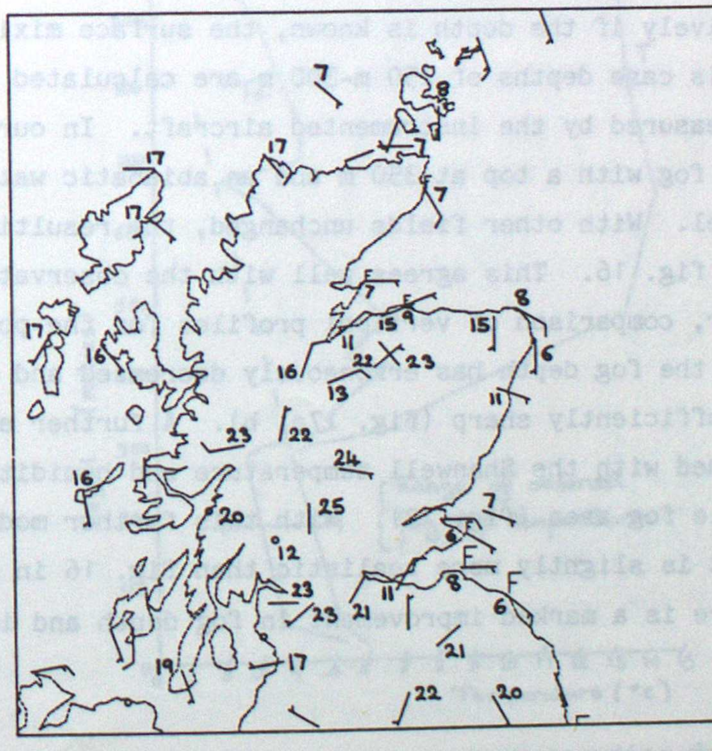

Figure 11. Observed temperature, wind and fog 1500 GMT 27/4/1984 (F-visibility <200 m, f-visibility <1000m)

Use of an objective analysis scheme to correct the initial fog distribution made matters worse since there are no observations over most of the sea (fig. 10) where there should be fog and all land stations report fog which is in fact confined to a narrow coastal strip. The resulting analysis remained deficient of fog over the sea but had most of Scotland covered. A forecast from this initialisation produced similar results to those obtained above since the shallow fog over land was soon dispersed by solar heating.

No attempt was made in this study to use the satellite imagery objectively. However, the difficulties are illustrated in figs. 13, 15. Figure 13 shows the midnight radiosonde ascent from Shanwell (see fig. 8) on the east coast of Scotland. It is representative of the air mass containing the fog with a mixed layer up to nearly 300 metres and then a sharp inversion. Figure 14 shows the calibrated fog top temperatures derived from the 0830 GMT AVHRR imagery. Over most of the area, these temperatures are colder than the base of the inversion at Shanwell, indicating a deeper fog. However, used in an objective scheme, these temperatures would all be assigned to a higher level (near 750 mb) at which the temperature did match. Clearly an intelligent system or human analyst is needed to correctly interpret these data. Fig. 15 shows liquid water paths deduced from the fog albedo. With the knowledge that the fog is well mixed and hence has an adiabatic profile, the depth can be derived, or alternatively if the depth is known, the surface mixing ratio can be estimated. In this case depths of 250 m-300 m are calculated which are about 70% of those measured by the instrumented aircraft. In our experiment the analyst inserted fog with a top at 350 m and an abiabatic water profile from zero at sea level. With other fields unchanged, the resulting nine hour forecast is shown in fig. 16. This agrees well with the observations in figs. 9, 11. However, comparison of vertical profiles for the point marked x in fig. 8 shows that the fog depth has erroneously decreased and that the fog top inversion is insufficiently sharp (fig. 17a, b). A further experiment was therefore performed with the Shanwell temperature and humidity profiles imposed over the whole fog area (fig. 13). With this further modification, the 1500 GMT forecast is slightly more realistic than fig. 16 in its fog distribution and there is a marked improvement in fog depth and inversion intensity (fig. 17c).

We may conclude from this study that detailed predictions of the behaviour of sea fog are possible if adequate initialisation is provided, and that this is possible through the intelligent combination of theory, imagery, surface

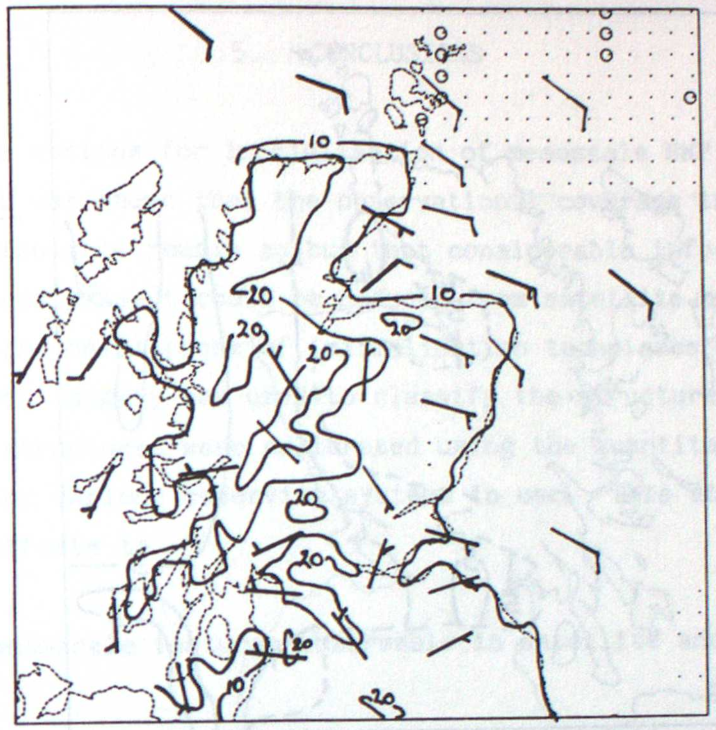

Figure 12. 9 hour forecast temperature, wind and fog for 1500 GMT 27/4/1984 from interpolated initialisation. (·-low cloud, o-fog)

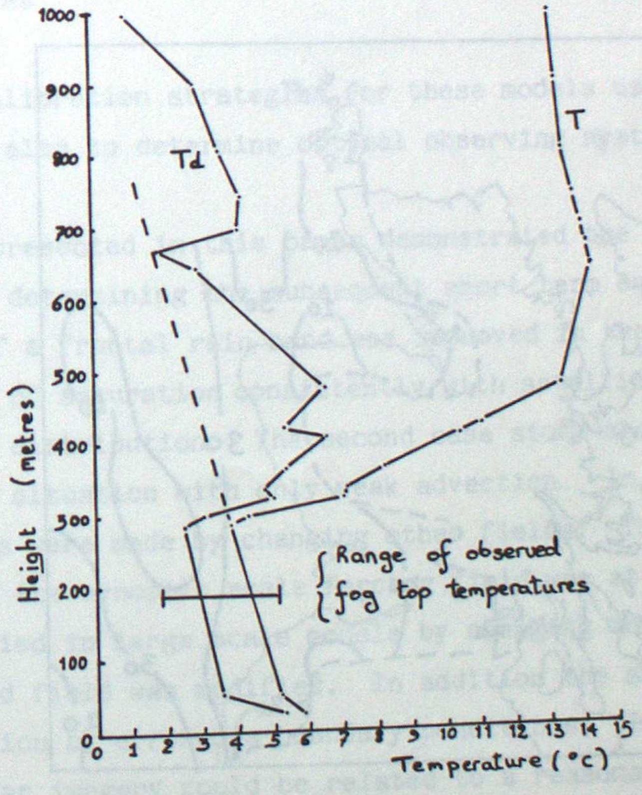

Figure 13. Detailed temperature and dew point sounding from Shanwell. 00 GMT 27/4/1984

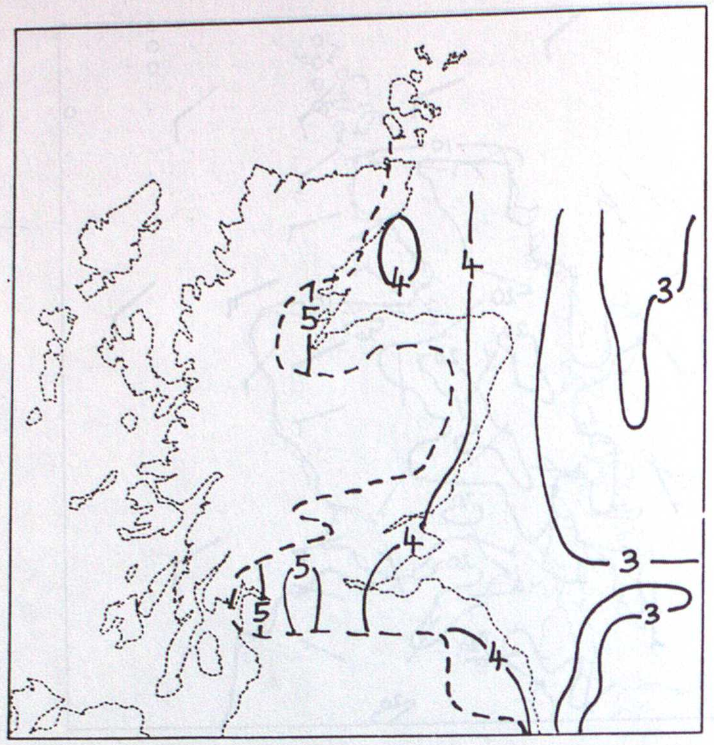

Figure 14. Fog top temperature distribution from NOAA-8 AVHRR imagery. 0833 GMT 27/4/1984

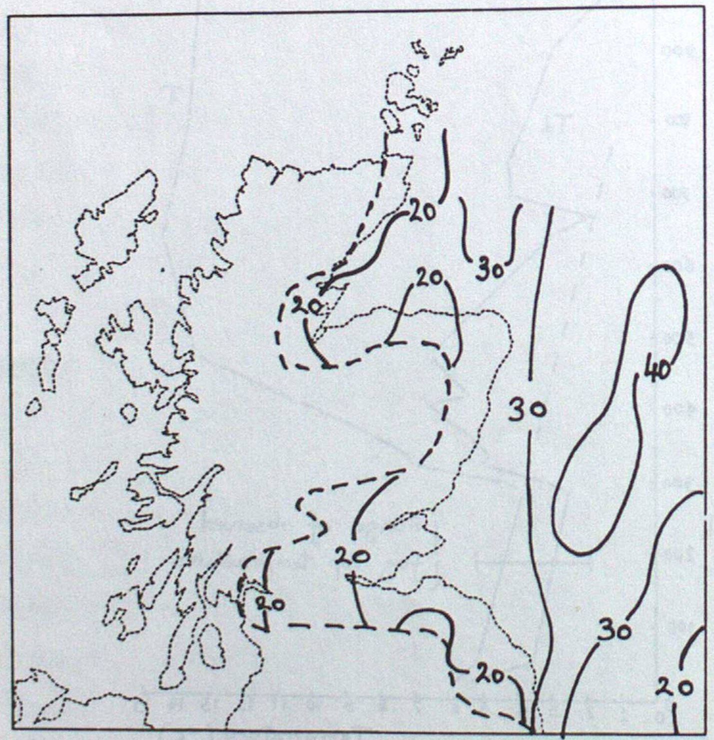

Figure 15. Liquid water path distribution (kg m^{-1}) deduced from NOAA-8 AVHRR imagery 0833 GMT 27/4/1984

observations and a single radiosonde ascent.

5. CONCLUSIONS

In this paper the options for initialisation of mesoscale NWP models were investigated. It was shown that the observational coverage is grossly inadequate and likely to remain so but that considerable information on the types of structures present could be deduced from satellite and radar imagery. A framework for the development of initialisation techniques was therefore suggested in which imagery was used to classify the structures present, and models of these structures were calibrated using the quantitative information available from the various observing systems in use. This strategy requires major research efforts to

(1) classify mesoscale features observable in satellite and radar imagery

(2) develop qualitative structural models of these features

(3) develop a quantitative dynamical and thermodynamical understanding of the structures

(4) determine calibration strategies for these models using available data sources and also to determine optimal observing systems

The case studies presented in this paper demonstrated the importance of the moisture field in determining the subsequent short term evolution. In one case the timing of a frontal rain band was improved in the first 6 hours by moving the region of saturation consistently with satellite imagery and the precipitation distribution. The second case study showed much longer term improvements in a situation with only weak advection. In both cases further minor improvements were made by changing other fields. The difference is that in the first case the synoptic scale forcing field was at fault and this is efficiently modified in large scale models by changing the temperature field. Here only the wind field was modified. In addition the small domain size led to rapid degradation by erroneous boundary conditions. In both cases the satellite and radar imagery could be related to a reasonably well understood phenomenon and the experiments mostly related to the calibration procedure. However it must be noted that many features, especially those dominated by convection, are not so well understood or even well described.

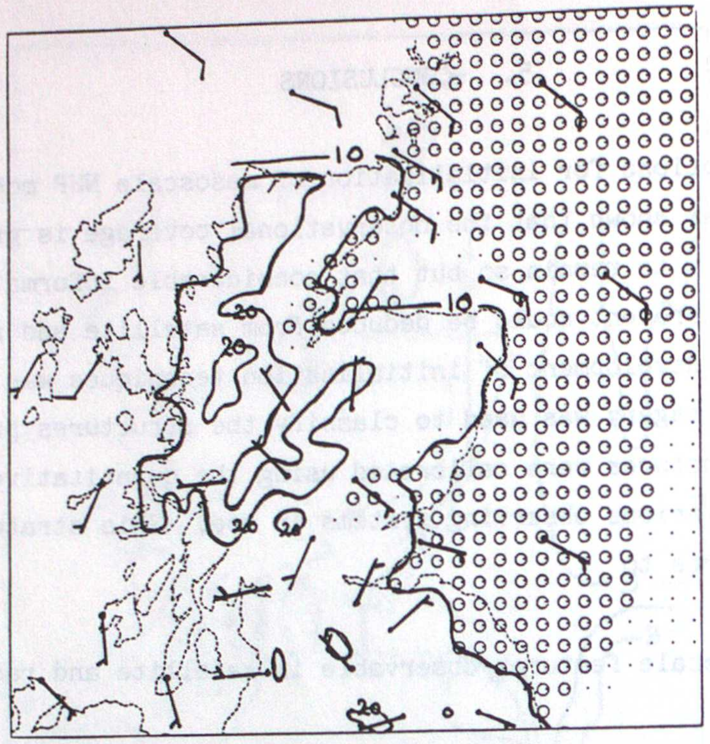

Figure 16. 9 hour forecast temperature, wind and fog for 1500 GMT 27/4/1984 from modified initialisation. (·-low cloud, o-fog)

6. ACKNOWLEDGEMENTS

I am grateful to Richard Barnes and Olive Hammon for the first case study and to Sue Ballard and Wilf Taylor for the second.

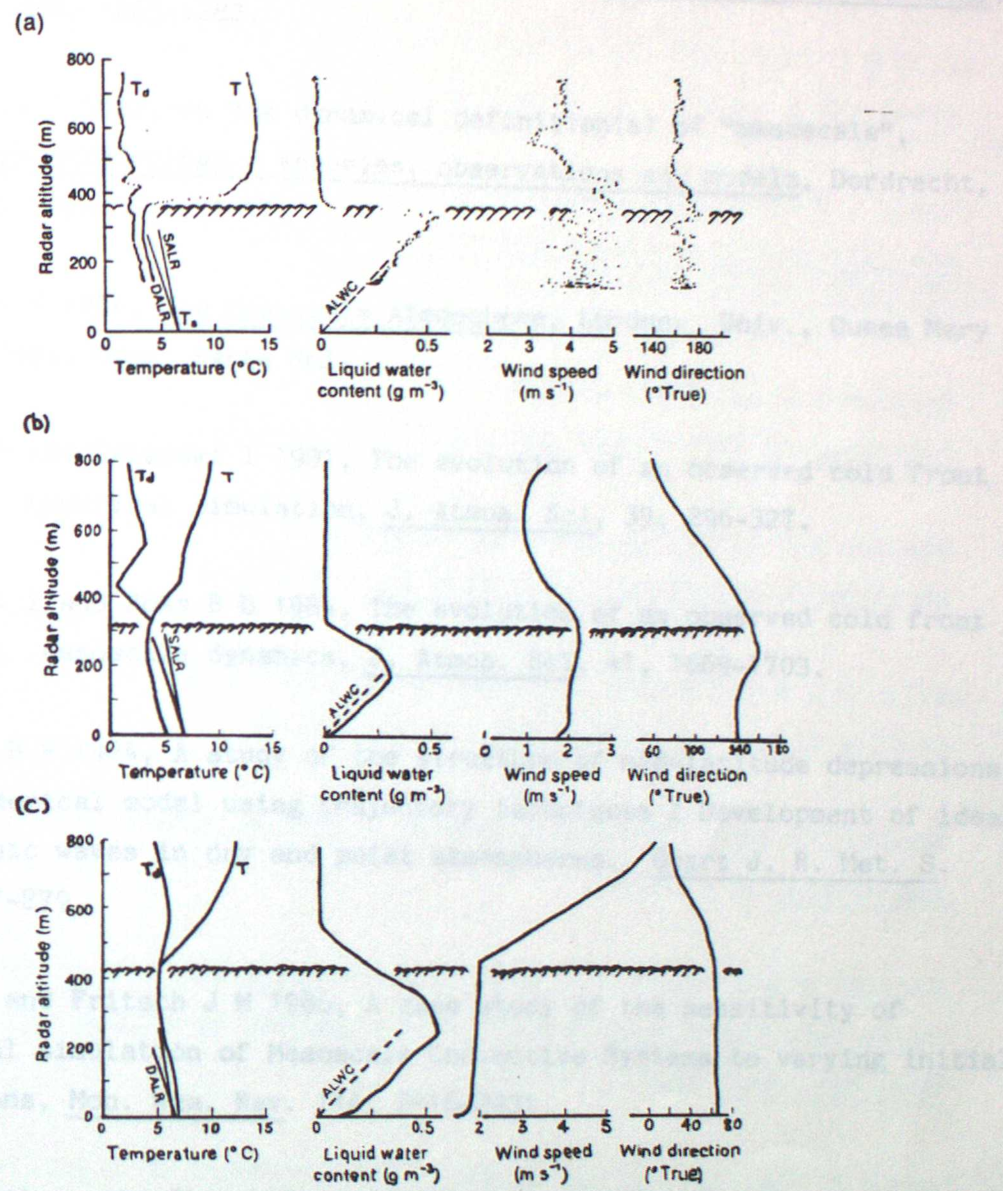

Figure 17. Profiles of temperature, dew point, liquid water and wind speed at x in fig. 8 for 1200 GMT 27/4/1984

(a) observed by instrumented aircraft

(b) 6 hour prediction from modified moisture initialisation

(c) 6 hour forecast from modified temperature and moisture initialisation

7. REFERENCES

1. Ligda M G H 1951, Radar storm observations, Compendium of Meteorology, Boston, AMS, 1265-1282.

2. Emanuel K A 1982, on the dynamical definition(s) of "mesoscale", Mesoscale Meteorology - theories, observations and models, Dordrecht, D Reidel Publ. Co., 1-11.

3. Atkinson B 1984, The Mesoscale Atmosphere, London: Univ., Queen Mary Coll., Dept. Geog. Earth Sci.

4. Ross B B and Orlanski I 1981, The evolution of an observed cold front Part I: numerical simulation, J. Atmos. Sci, 39, 296-327.

5. Orlanski I and Ross B B 1984, The evolution of an observed cold front Part II: mesoscale dynamics, J. Atmos. Sci, 41, 1669-1703.

6. Golding B W 1984, A study of the structure of mid-latitude depressions in a numerical model using trajectory techniques I Development of ideal baroclinic waves in dry and moist atmospheres. Quart J. R. Met. S. 110, 847-879.

7. Zhang D and Fritsch J M 1986, A case study of the sensitivity of numerical simulation of Mesoscale Convective Systems to varying initial conditions, Mon. Wea. Rev. 114, 2418-2431.

8. WMO Manual on the Global Observing System, WMO No. 544 Part 2, Attachment II. 3.

9. Nash J and Schmidlin F J 1987, Final report of the WMO International Radiosonde Intercomparison, WMO Instruments and Obs. Methods Rep. No. 30.

10. Eyre J R 1987, On systematic errors in satellite sounding products and their climatological mean values. Quart. J. R. Met. S. 113, 279-292.

11. Baer F and Tribbia J J 1977, On complete filtering of gravity modes through non-linear initialisation, Mon. Wea. Rev. 105, 1536-1539.

12. Machenhauer B 1977, On the dynamics of gravity oscillations in shallow water model with application to normal mode initialisation. Beitr. Phys. Atmos. 50, 253-271.

13. Leith C E 1980, Non-linear normal mode initialisation and quasi-geostrophic theory. J. Atmos. Sci. 37, 958-968.

14. Guymer L B 1978, Application of operational satellite imagery to synoptic analysis in the southern hemisphere. Melbourne, Bur, Met. Tech. Rep. No. 29.

15. Hoskins B J and Bretherton F P 1972, Atmospheric frontogenesis models, mathematical formulation and solution. J. Atmos. Sci. 27, 11-37.

16. Hoskins B J 1975, The geostrophic mementum approximation and the semi-geostrophic equations. J. Atmos. Sci. 233-242.

17. Cullen M J P and Purser R J 1984, An extended model of semi-geostrophic frontogenesis. J. Atmos. Sci. 41, 1477-1497.

18. Browning K 1985, Conceptual models of precipitation systems, ESA journal 9, 157-180.

19. Fiorino M and Warner T T 1981, Incorporating surface winds and rainfall rates into the initialisation of a mesoscale hurricane model. Mon. Wea. Rev. 109, 1914-1929.

20. Danard M 1985, on the use of satellite estimates of precipitation in initial analyses for numerical weather prediction. Atmos-Ocean 23 (1), 23-42.

21. Douglas C K M 1930, cold fogs over the sea, Meteorol. Mag. 65, 133-135.

22. Pilie R J et al 1979, the formation of marine fog and the development of fog-stratus systems along the Californian coast. J. Appl. Met. 18, 1275-1286.

23. Findlater J et al 1987, the Haar of North East Scotland, submitted to Quart. J. R. Met. S.

24. Tapp M C and White P W 1976, A non-hydrostatic mesoscale model, Quart. J. R. Met. S. 102, 227-296.

25. Carpenter K M 1979, An experimental forecast using a non-hydrostatic mesoscale model, Quart. J. R. Met. S. 105, 629-655.

26. Golding B W 1987, Short range forecasting over the United Kingdom using a mesoscale forecasting system, J. Met. Soc. Japan.

27. Bell R S and Dickinson A 1987, The Meteorological Office Operational Numerical Weather Prediction System, London: HMSO, Met. O. Sci. Pap No. 41.